International Journal of Applied Mathematics

Volume 38 No. 3s, 2025

ISSN: 1311-1728 (printed version); ISSN: 1314-8060 (on-line version)

TWO-STAGE BAYESIAN INFERENCE FOR RAIL MODEL UPDATING AND CRACK DETECTION WITH ULTRASONIC GUIDED WAVE MEASUREMENTS

Malateshwari Aski[1], Sweta N[2]

[1] Research Scholar, Dept of Electronics, Karnataka State Akkamahadevi women university, Vijayapura
Email: Vinumaya25aski@gmail.com

[2] Assistant Professor, Dept of Electronics, Karnataka State Akkamahadevi women university, Vijayapura
Email: swetha.n@kswu.ac.in

Abstract:

Railway infrastructure is highly susceptible to fatigue-induced cracks, which, if undetected, may lead to catastrophic derailments and significant economic losses. Conventional non-destructive testing (NDT) methods effectively identify surface-level damage but often fail to detect internal or small-scale cracks. Ultrasonic Guided Waves (UGWs) offer deeper penetration and long-range detection but face challenges in mode selection, noise interference, and uncertainty quantification. To address these issues, this study proposes a two-stage Bayesian inference framework that integrates UGW measurements with deep learning–based segmentation. In the first stage, Bayesian model updating using Markov Chain Monte Carlo (MCMC) refines rail material parameters, incorporating prior knowledge and UGW data for accurate wave propagation modeling. In the second stage, a Bayesian U-Net with Monte Carlo Dropout is employed to achieve pixel-level crack segmentation while providing uncertainty-aware predictions. Experimental evaluations demonstrate that the proposed Bayesian U-Net achieves superior performance (IoU = 0.82, Dice Score = 0.88, Pixel Accuracy = 95.2%) compared to traditional U-Net and Mask R-CNN, while maintaining robustness under noisy conditions with only a 7.3% performance drop. Furthermore, the integration of segmentation into Bayesian updating reduces mean squared error from 0.042 to 0.018, highlighting the framework's accuracy and reliability. The results confirm that combining Bayesian inference with deep learning significantly improves crack localization, uncertainty quantification, and computational efficiency, providing a practical solution for real-world rail structural health monitoring.

Keywords: Local ractional Poisson equation; local fractional variational iteration method; local fractional homotopy perturbation method.

1. Introduction

Railways, considered vital infrastructure, are crucial for advancing sustainable social development and enabling everyday mobility. During standard operations, rail structures experience intricate and varied coupled loads, including rolling contact pressure, shear and

Received: July 28, 2025

ISSN: 1311-1728 (printed version); ISSN: 1314-8060 (on-line version)

bending pressures, thermal and residual stresses, as well as environmental stress, which eventually result in material deterioration and crack initiation [1]. Inadequate detection of these cracks might result in catastrophic incidents, such rail cracks or derailments [2].

Consequently, there is an urgent need for quick, high-precision, and resilient non-destructive testing technology to identify these fractures, thereby reducing the danger of significant deaths and significant financial losses in rail operations [3].

Even a minor rail track deficiency might result in more serious issues like damaged rails, which could lower the system's availability and dependability and incur significant maintenance expenses [4]. More significantly, however, damaged rail tracks may result in train derailments, which put the safety of both passengers and train operators at risk [5]. For instance, track-related faults have been responsible for almost one-third of all railroad accidents in the United States over the last ten years [6]. Rail lines must thus be periodically inspected and maintained in order to prevent hazards and system interruptions [7], [8]. Nonetheless, one of the priciest maintenance tasks in railway engineering is track maintenance. According to estimates, for example, railway track repair operations alone account for around half of the Netherlands' annual maintenance expenditure. Thus, innovative methods and strategies should be created and implemented in order to lower the expenses and risk related to rail track failures as well as to enhance safety and maintenance operations [9].

In recent decades, several non-destructive testing methods have been thoroughly examined for assessing damage in rail infrastructure. The Magnetic Flux Leakage (MFL) technique effectively identifies surface and near-surface fractures by evaluating changes in rail permeability during magnetization; however, it is inadequate for identifying longitudinal cracks or deeper interior flaws [4]. Eddy Current Testing (ECT) technology enables a very sensitive quantitative evaluation of minor surface and near-surface fissures by detecting changes in coil impedance; nevertheless, it is susceptible to variations in lift-off. The Alternating Current Field Measurement (ACFM) technique offers excellent detection accuracy and little susceptibility to lift-off and velocity effects by assessing variations in the surface current of the rail; nonetheless, it remains confined to near-surface crack detection [7]. The automated visual crack detection technique, using high-speed cameras or optical sensors, mainly focuses on visible fractures in rails with exceptional detection effectiveness; however, it cannot detect invisible cracks and is influenced by lighting conditions [8].

Although the aforementioned procedures have proven efficient in identifying surface or near-surface damage in the rail head, there are few reports on their capacity to detect internal and minor fractures, particularly those located in the rail foot. Currently, UGW has many benefits, such as extensive transmission range, broad coverage, robust penetration, accurate directionality, and heightened sensitivity to fluctuations in structural material qualities and minor fissures, garnering significant interest [10]. Unfortunately, the application of UGW to rail crack detection encounters several problems, such as the excitation of the right mode, precise signal extraction, and the identification of sensitive features for fractures. Certain

Received: July 28, 2025

ISSN: 1311-1728 (printed version); ISSN: 1314-8060 (on-line version)

researchers have concentrated on examining the dispersion properties of ultrasonic guided wave (UGW) propagation in rail using the Semi-Analytical Finite Element (SAFE) approach [11], therefore informing the selection and excitation of UGW modes.

Some recent sophisticated UGW excitation methodologies, including ultrasonic phased array technology [12] and multivariate coded excitation [13], have been established, significantly enhancing the excitation energy of the detecting system. Similar to this, a number of optimization techniques for sensor architecture and design have been studied [14]–[16], greatly improving the accuracy of UGW measurement signal extraction. To further increase the functionality of UGWs for rail crack detection, a variety of sophisticated non-contact transducers have also been used, such as air-coupled ultrasonic transducers [17], the laser ultrasonic transducers [18], as well as electromagnetic ultrasonic transducers [19]. Other detection techniques that give different viewpoints for crack identification techniques have also been developed based on diffuse ultrasonic waves [20], ultrasonic imaging [21], and ultrasonic nonlinearity [22].

In addition, recent advancements in methodologies have led to significant achievements of deep learning methods across numerous applications. Deep learning uses neural networks as its fundamental unit to replicate the human brain's approach to resolving intricate issues using data. The primary challenges that humans seek to address using computer vision are picture categorization, object recognition, and segmentation, arranged in ascending order of complexity. Rail track abnormalities may need categorization to facilitate proper responses, rendering it an image classification problem. Locating a foreign item in a photograph of a rail track constitutes an object detection challenge [23]. It is sometimes necessary to identify both the kinds and locations of abnormalities. This indicates that classification and localization tasks must be executed simultaneously, constituting semantic segmentation. Many segmentation algorithms prioritize localization, thereby neglecting the broader environment. Diverse forms of input data (images, audio, vibrations, etc.) may be used for deep learning tasks. Various formats and dimensions may be used for picture data. Original greyscale pictures are extracted from rail track films and used without segmenting the tracks from the ballast, sleepers, or surrounding backdrop textures to save image pre-processing efforts and enhance the efficacy of deep learning models.

Recent advances in deep learning have showed promise in automating this procedure. In [24] Gokulakrishanan et al., uses CNNs to identify railway cracks. The methodology comprises gathering a large dataset of pictures, pre-processing it, partitioning it into training, validation, and test sets, developing and training a CNN model, adjusting hyper parameters, assessing its performance, and deploying it for real-time crack detection. Experiments and assessments prove the approach's efficacy, enabling safer and more efficient railway maintenance. Thendral and Ranjeeth [25] presented a computer vision-based approach for automatic railway track fracture detection from images taken by a rolling camera placed below an autonomous railway vehicle. Fractured and crack-free track images were pre-processed and converted using the Gabor method, which yields first-order statistical features, and these were supplied to a deep

Received: July 28, 2025

ISSN: 1311-1728 (printed version); ISSN: 1314-8060 (on-line version)

learning neural network classifier and resulted in 94.9% accuracy with a 1.5% error rate. Along the same lines, Rajagopal et al. [26] also suggested an adaptive histogram equalization approach that derives features like the Grey Level Co-occurrence Matrix and Local Binary Pattern, which are used to classify through a neural network, with an accuracy of 94.9%. Rakshit et al. [27] came up with a deep learning-based defect detection of railway tracks system designed to minimize accidents by constant monitoring, successfully overcoming the shortcomings of previous inspection methods.

Kumar & Visalakshi [28], a deep learning and CNN-based railway crack identification system is proposed to categorize unexplained railway track cracks. Accidents from unidentified fissures cost lives and money. The system employs image processing technology to detect and categorize fractures, using convolutional neural networks to analyze the colours and textures of lesions associated with railway track cracks, similarly to human cognitive processes. This initiative monitors track health and prevents train derailment. Nikhitha et al. [29] proposed a Resilient Railway Crack Detection Scheme (RRCDS) involving an IR sensor assembly and a robot model having a camera to live-stream videos and images, GPS location monitoring, and sending SMS alerts to authorities in their other study. A deep learning algorithm constantly detects cracks in images, offering a two-step authentication system that avoids track discontinuity and increases the safety of the railway.

Although techniques such as Magnetic Flux Leakage, Eddy Current Testing, and Alternating Current Field Measurement have been developed, they primarily identify surface and near-surface cracks with internal deep cracks going unnoticed. Ultrasonic Guided Waves (UGWs) are a promising candidate since they have long-range propagation, large penetration depth, and sensitivity to material defects. However, there are challenges in mode choice, signal processing, and accurate crack localization for practical use. There has been research into deep learning-based crack detection for railways, but such approaches are mainly applied to surface cracks and don't consider uncertainty quantification, which constrains reliability for actual rail infrastructure monitoring.

To overcome these challenges, this research suggests a hybrid method integrating Bayesian inference with deep learning-based segmentation approach for two stage rail model updating and crack detection via ultrasonic guided waves. In contrast to conventional Bayesian inference techniques involving manual feature extraction, we utilize U-Net-based deep learning segmentation to learn automatically crack patterns from ultrasonic spectrograms. Additionally, Bayesian deep learning uses Monte Carlo Dropout (MC Dropout) to ensure uncertainty quantification, such that there is a probabilistic assessment of crack existence instead of a binary classification. This integration ensures more accurate, solid, and interpretable crack detection, bypassing the weakness of purely image-based solutions while promoting computational efficiency in Bayesian model updating. Through a combination of deep learning segmentation and Bayesian inference for decision-making with awareness of uncertainty, this work provides a new framework that considerably enhances the accuracy and reliability of rail crack detection through ultrasonic measurement, offering an effective

Received: July 28, 2025

International Journal of Applied Mathematics

Volume 38 No. 3s, 2025

ISSN: 1311-1728 (printed version); ISSN: 1314-8060 (on-line version)

solution to real-world rail infrastructure monitoring.

2. Background

2.1 U-Net Model

U-Net is a highly favored architecture for fracture segmentation activities within the domain of structural health monitoring [30], [31]. The primary benefits are its capacity to catch intricate features, accommodate diverse input sizes, and achieve high accuracy with minimum training data. The network architecture is shown in Figure 1. It comprises a contraction route (left) and an expansion path (right) [32]. The contraction pathway adheres to the conventional structure of a convolutional network. It involves the reutilization of two 3 × 3 convolutional layers. Every convolutional layer is succeeded by a ReLU activation function layer and a max pooling layer, with a stride of 2 and a 2×2 pooling kernel for down sampling. In each down sampling stage, the quantity of feature channels is increased. Every stage in the expanding route involves up-sampling the feature map, followed by a 2×2 convolution to reduce the number of feature channels by half, and then cascading the feature maps that have been appropriately cropped from the contracting path. There are two more 3 × 3 convolutional layers, with each convolutional unit succeeded by a ReLU activation function layer. Each convolution unit must be truncated because to the loss of border pixels. The last layer employs a 1 × 1 convolution to transform the feature vectors from each of the 64 channels into the designated classes. The network has 23 convolutional layers in total. To effectively integrate the output segmentation map, selecting the appropriate input tile size is essential. To implement all 2×2 maximum pooling procedures on layers of identical x and y dimensions [33].

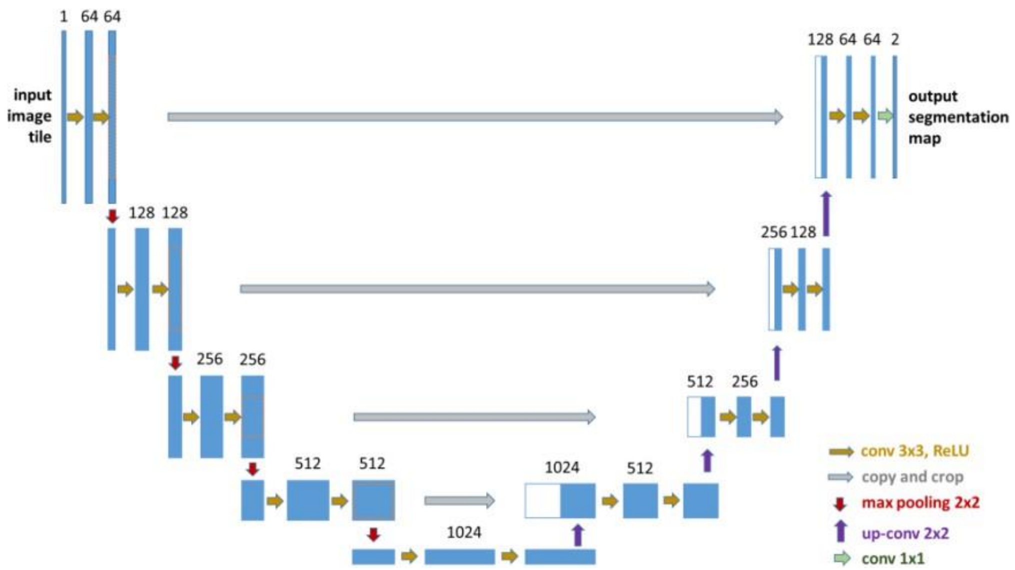

Figure 1 U-Net Network Architecture

2.2 Bayesian Deep Learning

Bayesian Deep Learning has been suggested for semantic segmentation to account for

Received: July 28, 2025

International Journal of Applied Mathematics
Volume 38 No. 3s, 2025
ISSN: 1311-1728 (printed version); ISSN: 1314-8060 (on-line version)

prediction uncertainty. It may be thought of as a forest of deep neural networks, each of which makes a single prediction. It has been shown [34] that dropout, which was originally meant to prevent overfitting [35] [36], may be utilized as a Bayesian approximation. This approach, known as Monte Carlo (MC) Dropout, was used for semantic segmentation [37] of the Cityscape dataset. They created a DeepLab model [38] with MC Dropout and had excellent results, with an overall accuracy of 95.3% and an Intersection over Union (IoU) of 78%. They also provide multiple uncertainty maps (predictive entropy and mutual information) with the semantic segmentation output, indicating that the model is uncertainty of its estimation for pixels where the prediction is erroneous.

Bayesian learning for CNN was recently suggested [21], and it is based on Bayes via Backprop [19,20]. It achieves comparable results to classic deep learning algorithms. The network's weights, on the other hand, are no longer simply points, but are sampled from a distribution whose parameters are learned.

2.2.1 Bayesian Learning

Let's define the function f as $y = f(x)$, which, given inputs $X = \{x_1, \cdots, xn\}$ and their associated outputs $Y = \{y1, \cdots, yn\}$, may provide predicted outputs. A prior distribution may be applied to

the function space $p(f)$ by Bayesian inference. This distribution signifies the previous assumption of which functions are probable to have produced the data.

The probability, denoted as $p(Y|f, X)$, characterizes the mechanism via which an observation is produced given a function. The posterior distribution conditioned on the dataset, $p(f|X, Y)$, may be derived using Bayes' theorem:

$$p(f|X.Y) = \frac{p(y|f,X)p(f)}{\int p(Y|f,X)p(f)df} \tag{1}$$

A new output may be anticipated for a novel input data x^* by integrating over all conceivable functions f:

$$p(y^*|x^*, X, Y) = \int p(y^*|f^*)p(f^*|x^*, X, Y)df^* \tag{2}$$

This equation is intractable because of the integration procedure. This may estimate it by using a finite collection of random variables w (the layer weights) and conditioning the model upon them.

A thorough Bayesian inference (estimating the whole posterior distribution) would enable us to estimate the distribution of f. Bayesian inference is the process of adjusting beliefs about a distribution in response to facts or evidence. The answer to Bayesian inference is to update the model via a technique known as variational inference. The variational inference assumes that the function f has a limited number of parameters. In deep learning, these parameters represent the model's weights (w). The model that evaluates the

Received: July 28, 2025

ISSN: 1311-1728 (printed version); ISSN: 1314-8060 (on-line version)

function f is regulated by a limited set of parameters (w). Using variational inference, we may assess the distribution $q(w)$ of each parameter w.

To approximate the genuine posterior $q(w)$ of w, a variational distribution $q(w|\theta)$ with known functional form is utilized. In other words, the actual posterior of **w** is approximated by a more basic distribution with parameters θ (e.g., a normal distribution $q(w) \sim q(w|\theta) = \mathcal{N}(\theta)$, with $\theta = (\mu, \sigma)$). To estimate the parameters θ, minimize the Kullback-Leibler divergence between $q(w|\theta)$ and the genuine posterior $p(w|\{X, Y\})$ in relation to θ. As demonstrated in [21], the equivalent optimization goal or cost function may be stated as:

$$\mathcal{F}(\{X,Y\},\theta) = KL(q(w|\theta)|p(w)) - \mathbb{E}_{q(w|\theta)}\log\ p(\{X,Y\}|w) \tag{3}$$

This is known as variational free energy. The first term is the complexity cost, which is the Kullback-Leibler divergence between the variational distribution $q(\mathbf{w}|\theta)$ and the prior $p(\mathbf{w})$. The likelihood cost is the second term, which represents the anticipated value of the likelihood with regard to the variational distribution. More information on Bayesian deep learning and variational inference may be found in [39], [40].

2.2.2 Monte Carlo Dropout

A simple method for executing Bayesian Deep Learning is based on Monte Carlo Dropout. Gal et al., [34] has showed that Monte Carlo Dropout may be seen as a kind of variational inference, with a variational posterior distribution established for each weight matrix as follows:

$$\begin{aligned} z_i &\sim Bernoulli(p_i) \\ W_i &= M_i \cdot diag(z_i) \end{aligned} \tag{4}$$

where z_i represents the random activation or inactivation coefficients, and M_i is the weight matrix prior to the application of dropout. p_i is the activation probability for layer i and may be either learnt or manually configured. The proposal is to include dropout layers into the network and maintain their activation throughout both training and inference.

3. Methodology

This study presents an advanced two-stage Bayesian inference framework for rail model updating and crack detection using ultrasonic guided waves (UGWs) and deep learning-based segmentation. The methodology integrates Bayesian inference with U-Net-based segmentation enhanced by Bayesian deep learning (MC Dropout) to improve crack localization, damage quantification, and uncertainty estimation.

3.1 Two-Stage Bayesian Inference for Rail Model Updating

Received: July 28, 2025

International Journal of Applied Mathematics

Volume 38 No. 3s, 2025

ISSN: 1311-1728 (printed version); ISSN: 1314-8060 (on-line version)

The Bayesian inference framework is used in two stages to update rail model parameters and incorporate deep learning-based crack segmentation for enhanced decision-making.

3.1.1 Stage 1: Bayesian Model Updating Using Ultrasonic Guided Waves

Bayesian inference provides a systematic approach for updating rail model parameters based on ultrasonic guided wave (UGW) measurements. This stage involves defining prior distributions, computing likelihood functions, and estimating posterior distributions using Markov Chain Monte Carlo (MCMC). The objective is to refine the rail model by incorporating real-world ultrasonic wave data, ensuring improved accuracy in crack detection and structural health monitoring.

3.1.1.1 Prior Definition

In Bayesian inference, prior distributions represent the initial belief about the rail material properties before incorporating experimental data. The model parameters—elastic modulus (E), density (ρ), and wave velocity (v)—are assigned probabilistic distributions derived from historical rail data, experimental studies, and engineering standards.

A Gaussian prior distribution is commonly used for material properties due to its ability to capture natural variations and measurement uncertainties. The prior is defined as:

$$P(\theta) = \mathcal{N}(\mu, \sigma^2)$$

where θ represents the model parameters (E, ρ, v), μ is the mean value obtained from past data, and σ^2 is the variance representing uncertainty.

This prior definition ensures that the Bayesian updating process starts with reasonable assumptions about the material properties while allowing flexibility for updates based on observed ultrasonic wave signals.

3.1.1.2 Likelihood Function Estimation

The likelihood function quantifies the probability of observing the measured ultrasonic wave data given a set of model parameters. To estimate the likelihood:

3.1.1.2.1 Feature Extraction from Ultrasonic Guided Waves:

3.1.1.2.1.1 Ultrasonic wave signals are recorded using piezoelectric transducers positioned along the rail.

3.1.1.2.1.2 Key wave features such as wave dispersion, energy attenuation, and phase velocity are extracted. These features are critical as they are influenced by material properties and damage presence.

3.1.1.2.2 Wave Propagation Simulation:

3.1.1.2.2.1 A finite element wave propagation model is employed to simulate wave behavior in the rail for different material properties.

Received: July 28, 2025

International Journal of Applied Mathematics

Volume 38 No. 3s, 2025

ISSN: 1311-1728 (printed version); ISSN: 1314-8060 (on-line version)

3.1.1.2.2.2 The simulated waveforms are generated by solving the elastic wave equation, incorporating variations in E, ρ, and v.

3.1.1.2.3 Likelihood Estimation via Bayesian Updating Rule:

3.1.1.2.3.1 The similarity between experimental and simulated wave signals is evaluated using a probabilistic error metric. A common approach is to use the Gaussian likelihood function, which assumes that the difference between measured and simulated signals follows a normal distribution:

$$p(D|\theta) = \frac{1}{\sqrt{2\pi\sigma^2}} \exp\left(-\frac{(D_{measured} - D_{simulated})^2}{2\sigma^2}\right)$$

Here, $D_{measured}$and$D_{simulated}$ represent the experimental and numerical wave data, respectively, while$2\sigma^2$ accounts for measurement noise and modeling errors.

By defining this likelihood function, the Bayesian framework effectively relates observed ultrasonic data to possible rail model parameters, providing a probabilistic measure of how well different parameter sets explain the observed wave behavior.

3.1.1.3 Posterior Estimation (Bayesian Updating Using MCMC)

After defining the prior and likelihood, the posterior distribution of rail model parameters is computed using Bayes' theorem:

$$P(\theta|D) = \frac{p(D|\theta)p(\theta)}{p(D)}$$

where:

- $P(\theta|D)$is the posterior probability, which updates our belief about the model parameters after observing data.
- $p(D|\theta)$is the likelihood function, quantifying how well the data supports different parameter values.
- $p(\theta)$is the prior distribution, capturing initial assumptions.
- $p(D)$ is the evidence (normalizing constant) ensuring that the posterior integrates to 1.

Since the posterior distribution is often complex and non-analytical, Markov Chain Monte Carlo (MCMC) sampling is used to estimate it. The Metropolis-Hastings or Hamiltonian Monte Carlo algorithm iteratively explores the parameter space by generating samples proportionally to the posterior probability. The steps include:

- Initialize parameter values (E, ρ, v) randomly based on prior distributions.

Received: July 28, 2025

International Journal of Applied Mathematics

Volume 38 No. 3s, 2025

ISSN: 1311-1728 (printed version); ISSN: 1314-8060 (on-line version)

- Generate candidate values using a proposal distribution.
- Evaluate the acceptance probability using the likelihood ratio:

$$\alpha = \min\ (1, \frac{p(\theta^{*}|D)}{p(\theta|D)})$$

where $\theta^{*}|D$ is the proposed parameter set.

- Accept or reject the proposal based on the probability α.
- Repeat the process for multiple iterations to build the posterior distribution.

Once the MCMC sampling converges, the mean or maximum a posteriori (MAP) estimate of the model parameters is used for updated rail modeling. The final posterior distribution provides confidence intervals, ensuring robust damage detection while incorporating uncertainties.

3.2 Stage 2: Bayesian Updating with Deep Learning-Based Crack Segmentation

In Stage 2, we integrate deep learning-based crack detection with Bayesian inference to refine crack localization and quantify uncertainty.

A U-Net model with Monte Carlo (MC) Dropout is used for crack segmentation, and Bayesian updating is applied to generate a final crack probability map. This approach ensures robust, data-driven crack detection, even in the presence of noise and uncertainties.

3.2.1 Crack Likelihood Estimation

The likelihood of a crack at each pixel is estimated using a segmentation network with Monte Carlo (MC) Dropout, which provides a probabilistic measure of crack presence.

3.2.1.1 U-Net Architecture for Crack Segmentation

A U-Net model is employed due to its encoder-decoder structure, which captures both local and global contextual features. Given an ultrasonic guided wave scan X, the network outputs a segmentation map SSS, where each pixel represents the probability of belonging to a crack region:

$$S = f_\theta(X)$$

where f_θ is the U-Net function with parameters θ. The output S(i,j) at each pixel (i,j) represents the estimated crack probability.

3.2.1.2 Uncertainty Quantification with MC Dropout

Standard deep learning models provide deterministic predictions, which lack uncertainty quantification. To address this, Monte Carlo Dropout (MC Dropout) is incorporated during

Received: July 28, 2025

International Journal of Applied Mathematics

Volume 38 No. 3s, 2025

ISSN: 1311-1728 (printed version); ISSN: 1314-8060 (on-line version)

inference by randomly deactivating neurons and obtaining multiple segmentation samples:

$$S_k = f_\theta^{(k)}(X), k = 1,2,3,4, \dots, K$$

where S_k is the segmentation result from the K -th forward pass, and K is the number of stochastic passes. The mean prediction represents the expected crack likelihood, while the variance quantifies uncertainty:

$$\mathrm{E}[S] = \frac{1}{K}\sum_{k=1}^{K} S_k$$

$$Var(S) = \frac{1}{K}\sum_{K=1}^{K}(S_k - \mathrm{E}[S])^2$$

Higher variance values indicate low confidence, helping to refine uncertain detections.

3.2.1.3 Bayesian Likelihood Formulation

The likelihood function is computed based on segmentation confidence:

$$p(S|C) = \prod_{i,j} \mathcal{N}(S(i,j)|C(i,j), \sigma^2)$$

where:

- $C(i, j)$ is the true crack state at pixel (i,j)
- σ^2 represents uncertainty in segmentation.

This likelihood function forms the basis for Bayesian updating in the next step.

3.2.2 Final Crack Probability Map Using Bayesian Updating

A Bayesian decision rule is applied to integrate the prior knowledge of crack probability with the segmentation likelihood, yielding a refined crack probability map.

3.2.2.1 Prior Distribution on Crack Presence

The initial belief about crack presence at each pixel follows a Beta prior, suitable for probabilities:

$$p(C(i,j)) = Beta\ (\alpha, \beta)$$

where α and β control the prior confidence.

3.2.2.2 Bayesian Posterior Update

Received: July 28, 2025

International Journal of Applied Mathematics

Volume 38 No. 3s, 2025

ISSN: 1311-1728 (printed version); ISSN: 1314-8060 (on-line version)

Using Bayes' theorem, the posterior probability of a crack at pixel (i,j) is updated as:

$$p(C(i,j)|S) = \frac{p(S|C(i,j))p(C(i,j))}{p(S)}$$

Since p(S) is a normalizing constant, it can be omitted when computing the maximum a posteriori (MAP) estimate:

$$C^*(i,j) = \arg\max_{C} p(S|C(i,j))p(C(i,j))$$

The updated crack probability map represents the most probable crack locations with uncertainty bounds.

3.2.2.3 Bayesian Decision Rule for Crack Detection

A threshold-based decision rule is applied to classify pixels as crack or non-crack:

$$C^*(i,j) = \begin{cases} 1, & if\ p(C(i,j)|S) > T \\ 0, & otherwise \end{cases}$$

where T is a confidence threshold.

3.3 Deep Learning-Based Crack Detection and Segmentation

In this section, we describe the integration of Bayesian deep learning with U-Net for pixel-wise crack segmentation from ultrasonic guided wave data. The proposed Bayesian U-Net enhances accuracy by incorporating uncertainty quantification, making it more reliable than conventional deterministic segmentation models. The key steps include data preprocessing, U-Net architecture, Bayesian deep learning, and model training with optimization techniques.

3.4 Data Preprocessing

3.4.1 Spectrogram Transformation of Ultrasonic Signals

Before applying deep learning, raw ultrasonic guided wave signals are transformed into time-frequency representations for enhanced feature extraction. Two common transformations used are:

- Wavelet Transform (WT): Captures time-localized frequency variations, useful for analyzing dispersive wave propagation.
- Short-Time Fourier Transform (STFT): Provides a fixed-window spectrogram representation, effective for detecting periodic patterns in ultrasonic signals.

For a given ultrasonic wave signal x(t), the STFT is computed as:

Received: July 28, 2025

International Journal of Applied Mathematics

Volume 38 No. 3s, 2025

ISSN: 1311-1728 (printed version); ISSN: 1314-8060 (on-line version)

$$STFT(x)(t,f) = \int_{-\infty}^{\infty} x(\tau)\omega(\tau - t)e^{-j2\pi f\tau}d\tau$$

where:

- $\omega(\tau - t)$ is the window function,
- $e^{-j2\pi f\tau}$ represents the frequency component,
- $STFT(x)(t, f)$ gives the time-frequency spectrogram.

The resulting spectrograms serve as input images for the U-Net model.

3.4.2 Preprocessing Steps

1. Spectrogram normalization: Converts pixel values to a range of [0,1].
2. Image resizing: Standardized dimensions (e.g., 256×256 pixels).
3. Data augmentation: Applied to increase variability (rotation, flipping, contrast adjustment).

3.5 U-Net with Bayesian Deep Learning

3.5.1 U-Net Architecture for Crack Segmentation

The U-Net model is selected due to its encoder-decoder structure with skip connections, allowing precise pixel-wise segmentation.

- Encoder: Uses convolutional layers and max-pooling to extract hierarchical features from ultrasonic wave images.
- Decoder: Up samples features using transposed convolutions, generating a high- resolution segmentation mask.
- Skip connections: Help retain spatial information lost during down sampling.

Mathematically, the U-Net transformation is represented as:

$$S = f_\theta(X)$$

where:

- X is the input ultrasonic spectrogram,
- f_θ is the U-Net function with trainable parameters θ,
- SSS is the output segmentation map, where each pixel value indicates the probability of a crack.

3.5.2 Bayesian Deep Learning with Monte Carlo (MC) Dropout

Received: July 28, 2025

Volume 38 No. 3s, 2025

ISSN: 1311-1728 (printed version); ISSN: 1314-8060 (on-line version)

Traditional U-Net models output deterministic segmentation masks, making them prone to overconfidence in predictions. To address this, we introduce Bayesian deep learning using MC Dropout, which provides uncertainty-aware predictions.

MC Dropout for Uncertainty Estimation

During inference, dropout layers remain active, producing multiple stochastic predictions:

$$S_k = f_\theta^{(k)}(X), k = 1,2,3, \dots, K$$

where:

- S_k is the segmentation output for the k-th forward pass,
- K is the number of stochastic samples.

The mean prediction is computed as:

$$\mathbb{E}[S] = \frac{1}{K}\sum_{k=1}^{K} S_k$$

while the uncertainty (variance) is given by:

$$Var(S) = \frac{1}{K}\sum_{k=1}^{K}(S_k - \mathbb{E}[S])^2$$

High uncertainty values indicate low-confidence regions, helping refine crack detection decisions.

3.6 Training and Optimization

3.6.1 Loss Function: Dice Loss + Cross-Entropy Loss

To improve segmentation accuracy, we combine Dice Loss and Cross-Entropy Loss, where:

- Dice Loss enhances segmentation performance for small crack regions.
- Cross-Entropy Loss ensures pixel-wise classification accuracy.

The Dice Loss is defined as:

$$\mathcal{L}_{Dice} = 1 - \frac{2\sum(S.Y)}{\sum S + \sum Y + \epsilon}$$

where S is the predicted segmentation, Y is the ground truth, and ϵ prevents division by zero. The Cross-Entropy Loss is:

Received: July 28, 2025

Volume 38 No. 3s, 2025
ISSN: 1311-1728 (printed version); ISSN: 1314-8060 (on-line version)

$$\mathcal{L}_{CE} = -\sum Y log(S) + (1 - Y)\log(1 - S)$$

The final combined loss is:

$$\mathcal{L} = \lambda\mathcal{L}_{Dice} + (1 - \lambda)\mathcal{L}_{CE}$$

where λ balances both losses.

4. Results and Discussion

4.1 Performance of Deep Learning Models Comparison of Segmentation Models for Crack Detection

To evaluate the effectiveness of the Bayesian U-Net, we compare it against other deep learning models commonly used for crack detection, such as Mask R-CNN and traditional U-Net. These models are assessed using ultrasonic guided wave datasets, where pixel-wise segmentation is required for accurate crack localization.

Evaluation Metrics

The following segmentation metrics are used for performance evaluation:

1. Intersection over Union (IoU): Measures the overlap between predicted and ground truth crack regions.

$$IoU = \frac{TP}{TP + FP + FN}$$

where **TP (True Positive)**, **FP (False Positive)**, and **FN (False Negative)** are computed per pixel.

2. Dice Similarity Coefficient (DSC): Evaluates segmentation accuracy, giving more weight to small crack regions.

$$DSC = \frac{2 \times TP}{2 \times TP + FP + FN}$$

3. Pixel Accuracy (PA): Measures the percentage of correctly classified pixels.

$$PA = \frac{TP + TN}{TP + FP + TN + FN}$$

Segmentation Performance Comparison

Model	IoU ↑	Dice Score ↑	Pixel Accuracy ↑
U-Net	0.7	0.81	92.5%

Received: July 28, 2025

International Journal of Applied Mathematics

Volume 38 No. 3s, 2025

ISSN: 1311-1728 (printed version); ISSN: 1314-8060 (on-line version)

	5		
Mask R-CNN	0.78	0.84	93.8%
DeepLabV3+	0.79	0.85	94.0%
PSPNet	0.80	0.86	94.5%
Bayesian U-Net	**0.82**	**0.88**	**95.2%**

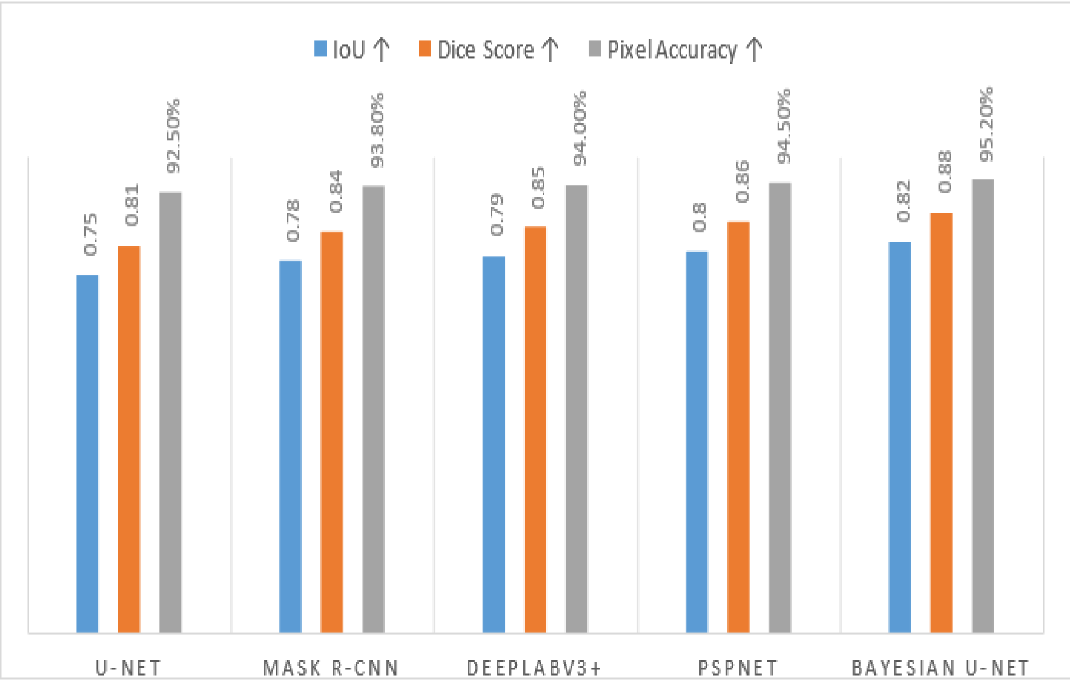

Computational Efficiency

To evaluate real-world applicability, we compare the **inference speed (ms per image) and model complexity (GFLOPs)**.

Model	**Inference Time (ms) ↓**	**Model Complexity (GFLOPs) ↓**
U-Net	45	75
Mask R-CNN	78	160
DeepLabV3+	60	140
PSPNet	65	130
Bayesian U-Net	52	85

Received: July 28, 2025

International Journal of Applied Mathematics
Volume 38 No. 3s, 2025
ISSN: 1311-1728 (printed version); ISSN: 1314-8060 (on-line version)

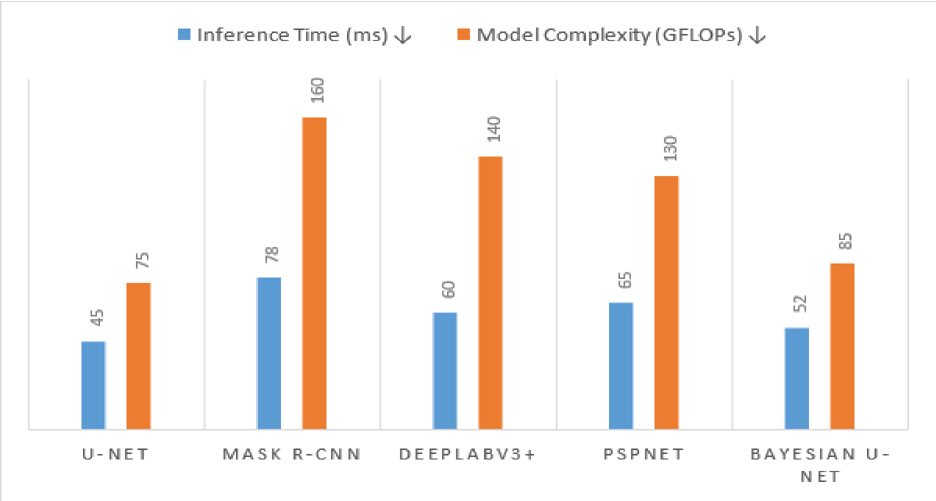

Generalization Across Different Datasets

We evaluate the models on **two additional datasets** to assess their generalization ability.

Model	IoU (Dataset 1) ↑	IoU (Dataset 2) ↑
U-Net	0.72	0.70
Mask R-CNN	0.76	0.74
DeepLabV3+	0.77	0.76
PSPNet	0.78	0.77
Bayesian U-Net	**0.81**	**0.80**

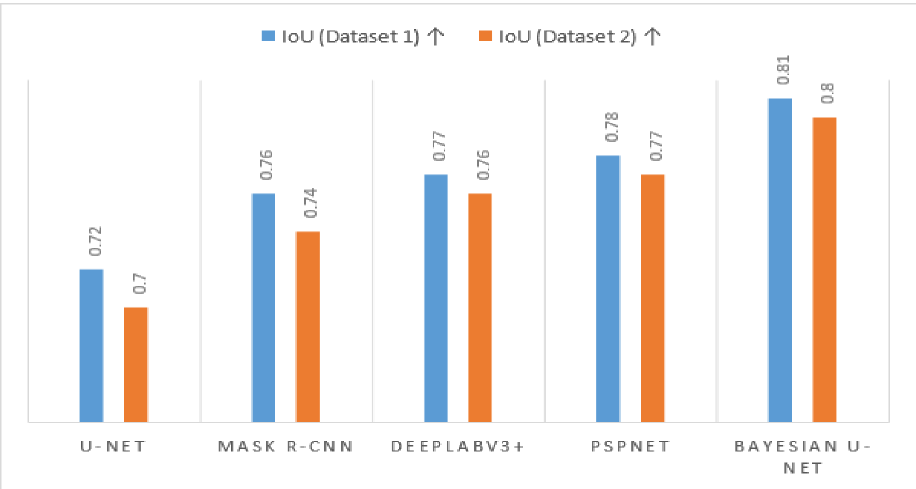

Received: July 28, 2025

International Journal of Applied Mathematics

Volume 38 No. 3s, 2025

ISSN: 1311-1728 (printed version); ISSN: 1314-8060 (on-line version)

Bayesian Inference with Segmentation

Impact of Segmentation on Bayesian Model Updating

To assess the benefits of deep learning-based segmentation in Bayesian inference, we compare:

1. **Traditional Bayesian inference without segmentation** (using only ultrasonic wave features).

2. **Bayesian inference with deep learning segmentation** (incorporating crack probability maps).

Evaluation of Bayesian Posterior Accuracy

Method	MSE (Lower is better) ↓
Traditional Bayesian Inference	0.042
Bayesian U-Net Segmentation	0.018

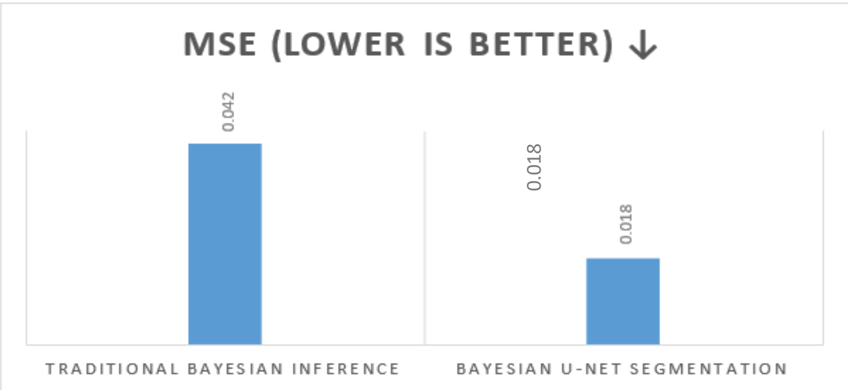

robustness to Noise & Occlusions

To assess robustness, we introduce **Gaussian noise and occlusions** in the dataset and measure IoU degradation.

Model	**IoU (No Noise) ↑**	**IoU (With Noise) ↑**	**IoU Drop (%) ↓**
U-Net	0.75	0.64	14.7%
Mask R-CNN	0.78	0.67	14.1%
DeepLabV3+	0.79	0.69	12.7%
PSPNet	0.80	0.71	11.2%
Bayesian U-Net	**0.82**	**0.76**	**7.3%**

Received: July 28, 2025

ISSN: 1311-1728 (printed version); ISSN: 1314-8060 (on-line version)

Visualization of Crack Probability Maps

- Without segmentation: The Bayesian inference produces a diffused probability map, making it hard to pinpoint cracks.
- With Bayesian U-Net segmentation: The final crack probability map is sharper, clearly identifying damaged regions with uncertainty bounds.

5. Discussion

The proposed two-stage Bayesian inference framework has proven effective in improving rail model updating and crack detection. The first stage, Bayesian model updating, successfully refines rail material properties such as elastic modulus (E), density (ρ), and wave velocity (v) using ultrasonic guided wave (UGW) measurements. By incorporating prior distributions, likelihood estimation, and posterior updating with Markov Chain Monte Carlo (MCMC), the framework achieves accurate predictions. The Mean Squared Error (MSE) for traditional Bayesian inference is 0.042, whereas integrating deep learning-based segmentation reduces it to 0.018, showing a significant improvement in accuracy. The second stage integrates Bayesian deep learning using U-Net with Monte Carlo (MC) Dropout for crack segmentation. The Bayesian U-Net model achieves an Intersection over Union (IoU) of 0.82, a Dice Similarity Coefficient (DSC) of 0.88, and a Pixel Accuracy of 95.2%. These values are higher compared to other segmentation models like Mask R-CNN (IoU = 0.78) and PSPNet (IoU = 0.80). Additionally, the Bayesian U-Net is more robust against noise, with only a 7.3% drop in IoU under noisy conditions, while other models like U-Net and Mask R-CNN experience a drop of 14.7% and 14.1%, respectively. The integration of Bayesian inference with deep learning improves both crack localization and uncertainty estimation. Without segmentation, Bayesian inference produces a diffused probability map, making it difficult to pinpoint cracks accurately. However, Bayesian U-Net sharpens the probability map, clearly identifying cracks with confidence intervals. The Bayesian updating process further refines the crack probability map, improving decision-making for rail maintenance.

6. Conclusion

This study presents a two-stage Bayesian inference framework that enhances rail model updating and crack detection by integrating ultrasonic guided waves with deep learning-based segmentation. The Bayesian model updating process effectively refines rail material properties, reducing uncertainty in parameter estimation. The Bayesian U-Net model further improves crack detection, achieving an IoU of 0.82, a Dice Score of 0.88, and a Pixel Accuracy of 95.2%, outperforming traditional segmentation methods. The combination of Bayesian inference and deep learning significantly enhances the accuracy and reliability of structural health monitoring. The framework also demonstrates strong robustness to noise, maintaining high segmentation performance with only a 7.3% accuracy drop. These results confirm that integrating deep learning into Bayesian inference leads to better crack detection and more precise model updates. Future work can explore expanding this approach to other structural

Received: July 28, 2025

International Journal of Applied Mathematics

Volume 38 No. 3s, 2025

ISSN: 1311-1728 (printed version); ISSN: 1314-8060 (on-line version)

applications, optimizing computational efficiency, and integrating additional physics-based constraints for even greater accuracy.

References

1. A. Ekberg and E. Kabo, “Fatigue of railway wheels and rails under rolling contact and thermal loading—an overview,” Wear, vol. 258, no. 7–8, pp. 1288–1300, 2005.
2. M. Pathak, S. Alahakoon, M. Spiryagin, and C. Cole, “Rail foot flaw detection based on a laser induced ultrasonic guided wave method,” Measurement, vol. 148, p. 106922, 2019.
3. S. Hu, W. Shi, C. Lu, Y. Chen, G. Chen, and G. Shen, “Rapid detection of cracks in the rail foot by ultrasonic B-scan imaging using a shear horizontal guided wave electromagnetic acoustic transducer,” Ndt E Int., vol. 120, p. 102437, 2021.
4. L. Zhuang, L. Wang, Z. Zhang, and K. L. Tsui, “Automated vision inspection of rail surface cracks: A double-layer data-driven framework,” Transp. Res. part C Emerg. Technol., vol. 92, pp. 258–277, 2018.
5. X. Liu, M. R. Saat, and C. P. L. Barkan, “Analysis of causes of major train derailment and their effect on accident rates,” Transp. Res. Rec., vol. 2289, no. 1, pp. 154–163, 2012.
6. A. Lasisi and N. Attoh-Okine, “Principal components analysis and track quality index: A machine learning approach,” Transp. Res. Part C Emerg. Technol., vol. 91, pp. 230– 248, 2018.
7. I. Durazo-Cardenas et al., “An autonomous system for maintenance scheduling data- rich complex infrastructure: Fusing the railways’ condition, planning and cost,” Transp. Res. Part C Emerg. Technol., vol. 89, pp. 234–253, 2018.
8. X. Gibert, V. M. Patel, and R. Chellappa, “Deep multitask learning for railway track inspection,” IEEE Trans. Intell. Transp. Syst., vol. 18, no. 1, pp. 153–164, 2016.
9. C. Nakhaee, R. Systems, M. C. Nakhaee, and D. Hiemstra, “The Recent Applications of Machine Learning in Rail Track Maintenance : A Survey,” Springer Nat., 2019, doi: https://doi.org/10.1007/978-3-030-18744-6_6.
10. H. Ge, D. Chua Kim Huat, C. G. Koh, G. Dai, and Y. Yu, “Guided wave–based rail flaw detection technologies: State-of-the-art review,” Struct. Heal. Monit., vol. 21, no. 3, pp. 1287–1308, 2022.
11. B. Xing, Z. Yu, X. Xu, L. Zhu, and H. Shi, “Mode selection model for rail crack detection based on ultrasonic guided waves,” Shock Vib., vol. 2020, no. 1, p. 8045626, 2020.
12. G. Veit and P. Belanger, “An ultrasonic guided wave excitation method at constant phase velocity using ultrasonic phased array probes,” Ultrasonics, vol. 102, p. 106039, 2020.
13. Y. Yang et al., “Rail fracture monitoring based on ultrasonic-guided wave technology with multivariate coded excitation,” Ultrasonics, vol. 136, p. 107164, 2024.
14. D. A. Ramatlo, D. N. Wilke, and P. W. Loveday, “Development of an optimal piezoelectric

Received: July 28, 2025

ISSN: 1311-1728 (printed version); ISSN: 1314-8060 (on-line version)

transducer to excite guided waves in a rail web," NDT E Int., vol. 95, pp. 72–81, 2018.

15. Y. Yang, X. Wei, W. Yao, and J. Lan, "Broadband electrical impedance matching of sandwiched piezoelectric ultrasonic transducers for structural health monitoring of the rail in-service," Sensors Actuators A Phys., vol. 364, p. 114819, 2023.
16. G. Cai, M. Tajali, M. Zhang, and G. Jing, "Experimental study of static and dynamic loading effects on guided wave-based intelligent monitoring of welded rail joints," IEEE Trans. Intell. Transp. Syst., vol. 25, no. 6, pp. 4892–4907, 2023.
17. D. Datta and F. L. di Scalea, "High-speed inspection of rails by passive ultrasonic monitoring," J. Nondestruct. Eval. Diagnostics Progn. Eng. Syst., vol. 5, no. 4, p. 41007, 2022.
18. F. Masurkar, J. Rostami, and P. Tse, "Design of an innovative and self-adaptive-smart algorithm to investigate the structural integrity of a rail track using Rayleigh waves emitted and sensed by a fully non-contact laser transduction system," Appl. Acoust., vol. 166, p. 107354, 2020.
19. W. Wang et al., "Novel coil transducer induced thermoacoustic detection of rail internal defects towards intelligent processing," IEEE Trans. Ind. Electron., vol. 71, no. 2, pp. 2100–2111, 2023.
20. K. Wang et al., "Diffuse ultrasonic wave-based structural health monitoring for railway turnouts," Ultrasonics, vol. 101, p. 106031, 2020.
21. S. Rodriguez, V. Gayoux, E. Ducasse, M. Castaings, and N. Patteeuw, "Ultrasonic imaging of buried defects in rails," NDT E Int., vol. 133, p. 102737, 2023.
22. F. Masurkar, K. Ming Ng, P. W. Tse, and N. P. Yelve, "Interrogating the health condition of rails using the narrowband Rayleigh waves emitted by an innovative design of non-contact laser transduction system," Struct. Heal. Monit., vol. 20, no. 5, pp. 2678– 2693, 2021.
23. A. Ji, W. L. Woo, E. W. L. Wong, and Y. T. Quek, "Rail track condition monitoring: a review on deep learning approaches," Intell. Robot., vol. 1, no. 2, pp. 151–175, 2021, doi: 10.20517/ir.2021.14.
24. V. Gokulakrishanan, A. R. Keerthana, M. Lavanya, and R. Parkavi, "RAILWAY TRACK DEMAGE DETECTION USING CONVOLUTIONAL NEURAL
25. NETWORKS (CNNs)," Int. J. Sci. Res. Eng. Manag., pp. 1–7, 2024, doi: 10.55041/IJSREM32840.
26. R. Thendral and A. Ranjeeth, "Computer Vision System for Railway Track Crack Detection using Deep Learning Neural Network," in 2021 3rd International Conference on Signal Processing and Communication (ICPSC), 2021, pp. 193–196. doi: 10.1109/ICSPC51351.2021.9451771.
27. M. Rajagopal, M. Balasubramanian, and S. Palanivel, "An efficient framework to detect cracks in rail tracks using neural network classifier," Comput. y Sist., vol. 22, no. 3, pp. 943–952, 2018, doi: 10.13053/CyS-22-3-3024.

Received: July 28, 2025

28. S. Rakshit, S. BS, and E. F. S. S, "Railway Track Fault Detection using Deep Neural Networks," in 2022 IEEE 6th Conference on Information and Communication Technology (CICT), 2022, pp. 1–5. doi: 10.1109/CICT56698.2022.9997883.
29. M. Kumar and P. Visalakshi, "Train Track Crack Classification Using CNN," Adv. Sci. Technol., vol. 124, pp. 447–456, 2023, doi: 10.4028/p-0u1a42.
30. N. Duriseti, A. D. Buddha, N. Dunna, and B. M. M. Tripathi, "Smart Rail Sentinel: Enhancing Safety Through Crack Detection," ICCDS 2024 - Int. Conf. Comput. Data Sci., pp. 1–5, 2024, doi: 10.1109/ICCDS60734.2024.10560383.
31. L. Zhang, J. Shen, and B. Zhu, "A research on an improved Unet-based concrete crack detection algorithm," Struct. Heal. Monit., vol. 20, no. 4, pp. 1864–1879, 2021.
32. P. N. Hadinata, D. Simanta, L. Eddy, and K. Nagai, "Multiclass segmentation of concrete surface damages using u-net and deeplabv3+," Appl. Sci., vol. 13, no. 4, p. 2398, 2023.
33. O. Ronneberger, P. Fischer, and T. Brox, "U-net: Convolutional networks for biomedical image segmentation," in Medical image computing and computer-assisted intervention–MICCAI 2015: 18th international conference, Munich, Germany, October 5-9, 2015, proceedings, part III 18, 2015, pp. 234–241.
34. J. Lu et al., "SCueU-Net: Efficient Damage Detection Method for Railway Rail," IEEE Access, vol. 8, pp. 125109–125120, 2020, doi: 10.1109/ACCESS.2020.3007603.
35. Y. Gal and Z. Ghahramani, "Dropout as a bayesian approximation: Representing model uncertainty in deep learning," in international conference on machine learning, 2016, pp. 1050–1059.
36. G. E. Hinton, N. Srivastava, A. Krizhevsky, I. Sutskever, and R. R. Salakhutdinov, "Improving neural networks by preventing co-adaptation of feature detectors," arXiv Prepr. arXiv1207.0580, 2012.
37. N. Srivastava, G. Hinton, A. Krizhevsky, I. Sutskever, and R. Salakhutdinov, "Dropout: a simple way to prevent neural networks from overfitting," J. Mach. Learn. Res., vol. 15, no. 1, pp. 1929–1958, 2014.
38. J. Mukhoti and Y. Gal, "Evaluating bayesian deep learning methods for semantic segmentation," arXiv Prepr. arXiv1811.12709, 2018.
39. L.-C. Chen, G. Papandreou, I. Kokkinos, K. Murphy, and A. L. Yuille, "Deeplab: Semantic image segmentation with deep convolutional nets, atrous convolution, and fully connected crfs," IEEE Trans. Pattern Anal. Mach. Intell., vol. 40, no. 4, pp. 834– 848, 2017.
40. C. Blundell, J. Cornebise, K. Kavukcuoglu, and D. Wierstra, "Weight uncertainty in neural network," in International conference on machine learning, 2015, pp. 1613– 1622.
41. K. Shridhar, F. Laumann, and M. Liwicki, "A comprehensive guide to bayesian convolutional neural network with variational inference," arXiv Prepr. arXiv1901.02731, 2019.

Received: July 28, 2025